

---

## ARTICLE

---

# A simple treatment of increased gap due to fuel assembly bowing through correction of cross sections

Akio Yamamoto <sup>a\*</sup>, Tomohiro Endo <sup>a</sup>,

Hiroaki Nagano <sup>b</sup> Yasunori Ohoka <sup>b</sup> and Kento Yamamoto <sup>b</sup>

<sup>a</sup>*Nagoya University, Furo-cho, Chikusa-ku, Nagoya, Japan, 464-8603;*

<sup>b</sup>*Nuclear Fuel Industries, Ltd., Kumatori-cho, Sennan-gun, Osaka, Japan, 590-0481*

### Acknowledgments

This work was supported in part by the JSPS KAKENHI under Grant-in-Aid for Scientific Research (C) (16K06956).

Increased fuel assembly gap due to bowing in commercial LWRs has an impact on local pin-power distribution due to increased local moderation. In order to consider the effect of increased assembly gap without explicit consideration of increased gap width, a correction method of cross sections in the gap region is proposed. In this cross section correction method, the average chord length of gap region is preserved to capture the effect of increased gap width. The validity of the present method is confirmed by verification calculations in a single assembly and 5x5 assemblies geometries using the GENESIS code, which is a transport code based on the method of characteristics.

***Keywords; Assembly bowing, assembly gap, peaking factor, cross section correction, GENESIS, MOC***

---

\*Corresponding author. Email: a-yamamoto@energy.nagoya-u.ac.jp

## 1 **1. Introduction**

2 Fuel assemblies are bowed during burnup in a reactor core, due to various reasons  
3 such as irradiation growth of cladding materials [1-3]. Variation in the assembly gap  
4 dimension affects pin power peaking factor since local moderation ratio around the assembly  
5 gap region is changed [1-3]. If the assembly gap increases comparing to its nominal value,  
6 adjacent pin power increases due to increased local moderation. The locally increased pin  
7 power reduces thermal margin thus this effect is considered as a safety margin. Therefore,  
8 estimation of power peaking factor variation due to change of assembly gap is one of the  
9 important issues in the core safety analysis. This issue has been recognized for a long time  
10 and some of the core design codes have the capability to evaluate the effect of assembly  
11 bowing on core characteristics [4, 5].

12 Recently, high-fidelity core simulations incorporating explicit heterogeneous core  
13 geometry are becoming familiar using the planar method of characteristics (MOC) or other  
14 methods such as the Legendre polynomial Expansion of Angular Flux (LEAF) method [6-9].  
15 Let us consider the modeling capability of these high-fidelity simulation codes for the  
16 assembly bowing. A bowed fuel assembly can be modeled as radially offset fuel assemblies in  
17 a core. In principle, since these simulation codes are based on the MOC or similar method,  
18 such deformation can be explicitly modeled. However, in reality, it would be cumbersome  
19 since the direct neutron path linking (DNPL, sometimes called the modular ray trace) method  
20 may be used [10]. In the DNPL method, a whole geometry is covered by square, rectangular,  
21 or hexagonal frames having the identical dimension. When an offset fuel assembly protrudes  
22 its own frame, parts of two fuel assemblies coexist in the adjacent frame. Such a situation  
23 would require cumbersome input data preparation since the geometry depends on the offset  
24 dimension, which is different for every fuel assemblies in a core. Furthermore, a dedicated  
25 edit for the pin- and assembly-power distribution would be necessary since a fuel assembly  
26 would span different frames used in DNPL. Otherwise, in order to make the input data simple,

1 the offset size of a fuel assembly may be limited [11]. A fuel assembly usually bows  
2 three-dimensionally, thus the magnitude of offset varies along the axial direction. Such a  
3 situation also poses difficulties since some of the core analysis codes utilize the extruded  
4 geometry for axial direction [9].

5 In order to address the above issue, a simplified treatment is proposed. In the present  
6 method, the nominal (non-offset) geometry is used in a calculation while the effect by offset  
7 geometry is captured by correction of cross sections at the gap water region between fuel  
8 assemblies. In a nutshell, a variation of gap water size between assemblies is converted to the  
9 variation of cross sections of the gap water region to preserve the transmission probability in  
10 the gap water region. Only cross sections in the gap water region between fuel assemblies are  
11 corrected and the cross sections inside fuel assemblies (e.g. fuel pin cell) are not corrected.  
12 PWR fuel assemblies are mainly considered in the present study, but the present method can  
13 be applied to other fuel assembly types.

14 In section 2, the theory behind the present method is described. The verification results  
15 will be shown in section 3. Finally, concluding remarks will be summarized in section 4.

16

## 17 **2. Theory**

### 18 ***2.1. Relation between Geometry Deformation and Cross Section Correction***

19 The present method is inspired by the previous works [12, 13]. In the reference [12],  
20 geometry variation due to thermal expansion is incorporated by the correction of cross  
21 sections while maintaining the geometry unchanged. The reference [13] utilizes the concept of  
22 “virtual number density” to handle perturbation of region boundaries. These works suggest  
23 that some of the geometry variations can be treated by the correction on cross sections or  
24 number densities.

25 Here, the one-group neutron transport equation for MOC is considered:

$$\frac{d\psi}{ds} + \Sigma_t \psi = \frac{1}{4\pi} \left( \Sigma_s \phi + \frac{1}{k} \nu \Sigma_f \phi \right), \quad (1)$$

1 where  $\psi$ : angular flux,  $\phi$ : scalar flux,  $s$ : coordinate in neutron flight direction,  $\Sigma_t$ : total  
 2 cross section,  $\Sigma_s$ : scattering cross section,  $\nu \Sigma_f$ : production cross section,  $k$ : effective  
 3 multiplication factor. Note that extension to the multi-group transport equation is easy without  
 4 loss of generality.

5 A new coordinate is introduced as:

$$\tilde{s} = \frac{1}{f} s, \quad (2)$$

6 where  $f$  is a scaling factor. By substituting Equation (2) to Equation (1), Equation (3) is  
 7 obtained:

$$\frac{d\psi}{d\tilde{s}} + f \Sigma_t \psi = \frac{1}{4\pi} \left( f \Sigma_s \phi + \frac{1}{k} f \nu \Sigma_f \phi \right). \quad (3)$$

8 Now the corrected cross sections are introduced as:

$$\tilde{\Sigma} = f \Sigma. \quad (4)$$

9 Finally, the following equation is obtained:

$$\frac{d\psi}{d\tilde{s}} + \tilde{\Sigma}_t \psi = \frac{1}{4\pi} \left( \tilde{\Sigma}_s \phi + \frac{1}{k} \nu \tilde{\Sigma}_f \phi \right). \quad (5)$$

10 The above formulation indicates that a variation of geometry is exactly captured by the  
 11 correction of cross sections in one-dimensional slab geometry. For example, let us consider an  
 12 increased gap region between fuel assemblies whose gap size is the twice of the nominal  
 13 value. In order to model this gap region as the nominal size, the cross sections in this region  
 14 are doubled in order to preserve the transmission probability at the gap region. Contrary, when  
 15 the gap size between assemblies is reduced to the half of the nominal value, the cross sections  
 16 of the gap region are halved in order to model this gap with the nominal size.

17 The assembly bow usually has offsets for  $x$ - and  $y$ -directions thus two-dimensional

1 deformation should be considered in principle. However, the assembly gap is narrow and can  
2 be considered as two independent one-dimensional deformations for  $x$ - and  $y$ -directions  
3 except for the corner gap region.

4 In the present method, only the cross sections at the gap water region are corrected and  
5 those inside a fuel assembly (e.g., fuel pin-cell) are not corrected.

6

## 7 **2.2. Correction in Corner Gap Region**

8 In the corner of assembly gap, the average chord length  $l$  calculated by  $l=4V/S$ , where  $V$   
9 and  $S$  are the volume and surface of the corner gap region, is considered as the “thickness” of  
10 this region. For example, when the nominal dimensions of corner gap are  $\Delta x$  and  $\Delta y$ , the  
11 average chord length is  $l = \frac{4\Delta x\Delta y}{2\Delta x+2\Delta y} = \frac{2\Delta x\Delta y}{\Delta x+\Delta y}$ . When the dimensions of gaps are increased to  
12  $\Delta\tilde{x}$  and  $\Delta\tilde{y}$ , the average chord length becomes to  $\tilde{l} = \frac{4\Delta\tilde{x}\Delta\tilde{y}}{2\Delta\tilde{x}+2\Delta\tilde{y}} = \frac{2\Delta\tilde{x}\Delta\tilde{y}}{\Delta\tilde{x}+\Delta\tilde{y}}$ . In this case, cross  
13 sections in the increased gap region are corrected by multiplying the factor  $f = \tilde{l}/l$  to the  
14 cross section in order to model this gap region with nominal size.

15 In a continuous energy Monte-Carlo code or an integrated core analysis code using  
16 number densities as the input data instead of the macroscopic cross section, the number  
17 densities are multiplied by the factor  $\tilde{l}/l$  instead of macroscopic cross section.

18 It should be noted that in the two-dimensional case, the total number of atoms in a  
19 corrected region is not preserved since the above correction just preserve the transmission  
20 probability or the optical length of a region. However, in the present application, the corner  
21 gap area is typically small thus no significant impact on the result is expected. The validity of  
22 this approximation is confirmed in the numerical calculations in the next section.

23 Variation of assembly gap size can be well modeled by one- or two-dimensional  
24 geometry. However, in principle, the present method can be directly applied to a variation in  
25 three-dimensional geometry. In the case of three-dimensional geometry, the chord length is  
26 calculated by its definition, i.e.,  $l=4V/S$ . The total number of atoms in a corrected region is not

1 preserved in a three-dimensional case as well as in a two-dimensional case as described  
2 above.

3

### 4 **3. Numerical Results**

5         Verification calculations are performed for the 2D single assembly geometries with  
6 offset positions and the 2D 5x5 multiple assemblies geometry that simulates part of a whole  
7 core. The present verification calculation aims to confirm the validity of the proposed  
8 methodology. Estimation of power peaking factor variation using actual plant data is out of  
9 the scope of this study. Comparison between the reference result considering explicit offset  
10 fuel assembly position (as is) with uncorrected cross section and the present result using the  
11 nominal (non-offset) geometry with the corrected cross section is major interest in this paper.

12

#### 13 ***3.1. Single Assembly Geometry***

14         The MOX-1 assembly specification in the KAIST benchmark problem [14] is used in the  
15 present study since a MOX fuel has a higher sensitivity to the size of assembly gap. In the  
16 original KAIST benchmark problem, no water gap is assigned between assemblies. However,  
17 in this section, the fuel assembly is assumed to be surrounded by narrow gap water whose  
18 nominal thickness is 0.1 cm. Thus, the nominal gap between assemblies is 0.2 cm and the  
19 assembly pitch is  $1.26 \times 17 + 0.1 \times 2 = 21.62$  cm. The 7-group heterogeneous macroscopic cross  
20 section provided in the benchmark problem is used. In an actual situation, effective cross  
21 sections of fuel rods adjacent to gap water depend on the thickness of gap due to the Dancoff  
22 effect. Variation of effective cross section due to increased or decreased gap size can be  
23 considered through the present method since the present method can be directly used for  
24 resonance calculations (e.g., Dancoff factor calculation, sub-group calculation, or ultra-fine  
25 group calculations). However, in the present study, the identical 7-group macroscopic cross  
26 section is used for all materials regardless of the gap size except for that of gap water. The

1 cross sections of gap water are corrected as described in the previous section.

2 Combination of gap water thickness around an assembly is shown in **Table 1** and **Figure**  
3 **1**. When the thickness of gap water increases, assembly pitch also increases. For example, the  
4 assembly pitches for the E0.1-S0.3 case are 21.62 cm and 22.02 cm for  $x$ - and  $y$ -directions,  
5 respectively. In the present method, the nominal gap water thickness (0.1cm) is used as is, but  
6 the cross section of gap water is corrected to preserve the average chord length (or  
7 transmission probability). In the case of E0.1-S0.3, cross sections in the south gap region is  
8 multiplied by factor 3 ( $=0.3/0.1$ ) while the nominal size (0.1cm) is used for the north, west,  
9 south, and east gap regions.

10 The GENESIS code [9] is used in the present calculation. Two-dimensional transport  
11 calculation based on MOC is used. Major calculation conditions are as follows:

- 12 •Ray trace width :0.005cm
- 13 •Number of azimuthal angles :64 (for  $2\pi$ )
- 14 •Number of polar angles :4 (TY, for  $\pi$ )
- 15 •Convergence criteria for flux : $10^{-4}$
- 16 •Convergence criteria for keff : $10^{-5}$

17 The reference and the present results are obtained by the following conditions:

- 18 •Reference: Uncorrected cross sections, offset geometry
- 19 •Present: Corrected cross sections, nominal geometry

20

21 (Table 1 Thickness of gap water around a fuel assembly (unit: cm))

22 (Figure 1 Layout of MOX fuel assembly and gap water)

23

24 The reflective boundary condition is used. Cross sections for gap water region are  
25 corrected by the method described in the theory section. In more detail, the ratio of gap size  
26 (offset/nominal) is multiplied all types of cross sections (*i.e.*, total, production, absorption,

1 and scattering) in the gap region.

2 **Table 2** summarizes k-infinities obtained by the reference and the present methods and  
3 their differences. The present method well captures variation of k-infinity due to increased  
4 gap width. **Figures 2** shows perturbations of pin-power (pin-by-pin fission rate) due to  
5 increased assembly gap, which are obtained by the reference calculations. The perturbation of  
6 pin-power is calculated by:

$$\Delta P = \frac{P_{Increased} - P_{nominal}}{P_{nominal}}, \quad (6)$$

7 where  $\Delta P$ ,  $P_{Increased}$ , and  $P_{nominal}$  are perturbation of pin-power, pin-powers in increased  
8 gap geometry, and pin-powers in nominal gap geometry. **Figure 2** clearly shows pin power  
9 around the increased gap region becomes higher as the size of gap water increases. **Figure 3**  
10 shows the difference of pin-powers between the reference and the present results calculated  
11 by (Present – Reference)/Reference. **Figures 4** and **5** show more detail comparison of  
12 pin-power distribution. From **Figure 2**, maximum variation of pin-powers due to variation of  
13 gap in the present calculation reaches approximately 20%. However, **Figure 3** shows the  
14 present method reproduces the reference pin-power distribution within 0.5% difference. These  
15 results indicate that the present model using the nominal geometry and the corrected cross  
16 sections well reproduces the reference result, which is obtained by the calculation using the  
17 explicit offset geometry and uncorrected cross sections.

18

19 (Table 2 Variation of k-infinity due to increased gap size)

20 (Figure 2 Perturbation of pin-power distribution due to increased assembly gap size (single  
21 assembly geometry) )

22 (Figure 3 Difference of pin-by-pin fission rate obtained by the reference and the present  
23 methods (single assembly geometry) )

24 (Figure 4 Comparison of pin-by-pin fission rate (Eastern boundary, from North-East corner to



1 South-East corner) )

2 (Figure 5 Comparison of pin-by-pin fission rate (Southern boundary, from West-South corner  
3 to East-South corner) )

### 5 **3.2. Multiple Assemblies Geometry**

6 In order to check the validity of the present method in a more realistic situation, offset  
7 fuel assemblies are modeled in a 5x5 assemblies geometry. The MOX-1 fuel assembly used in  
8 the previous section is also used. In this calculation, the nominal thickness of gap water  
9 around an assembly is assumed as 0.07cm. It means that the nominal gap size between  
10 assemblies is  $0.07 \times 2 = 0.14$  cm and nominal assembly pitch is  $1.26 \times 17 + 0.07 \times 2 = 21.56$  cm. As  
11 shown in **Figure 6**, the assemblies A and B are offset to the extreme left (west), *i.e.*, the gap  
12 between A and B, and the west gap of A are set to be 0.0 cm. The assemblies C, D, and E are  
13 offset to the extreme right (east). Thus the gap between C and D, D and E, and the east gap of  
14 E are set to be 0.0 cm. The gap size between assemblies B and C is 0.7 cm ( $=0.07 \times 2 \times 5$ ). In  
15 order to explicitly model this offset geometry, the geometries of assemblies A, B, C, D, and E  
16 are defined independently in the reference calculation.

17  
18 (Figure 6 5x5 assembly geometry with offset fuel assemblies.)

19  
20 The following GENESIS calculations are carried:

- 21 •Reference: Uncorrected cross sections, offset geometry (as is)
- 22 •Present: Corrected cross sections, nominal geometry (xs correction)

23 In addition, in order to estimate perturbation of pin-power due to increased assembly gap, a  
24 GENESIS calculation using the uncorrected cross section and the nominal geometry is carried  
25 out.

26 Calculation conditions of the GENESIS code are as follows:

- 1 •Ray trace width :0.05cm
- 2 •Number of azimuthal angles :32 (for  $2\pi$ )
- 3 •Number of polar angles :4 (TY, for  $\pi$ )
- 4 •Convergence criteria for flux : $10^{-4}$
- 5 •Convergence criteria for keff : $10^{-5}$

6 **Figure 7** shows the pin-by-pin fission rates for the increased gap (offset) configuration  
7 and the nominal configuration. The pin array within the horizontal yellow rectangle in **Figure**  
8 **6** is considered. Pin-by-pin fission rates significantly increase at the enlarged gap region  
9 (between assembly B and C) while decrease at reduced gap regions. **Figures 8** shows a  
10 variation of pin-powers within the horizontal yellow rectangle in **Figure 6**, calculated by  
11 Equation (6), due to increased assembly gap size. **Figures 9** corresponds to that within the  
12 vertical yellow frame in **Figure 6**. Again, pin-power around the increased gap region  
13 increases. Note that the change of k-infinity due to variation of gap size is small in this case,  
14 i.e., less than  $0.01\% \Delta k/k$ . Therefore, explicit comparison of k-infinity is not carried out for  
15 this case. **Figures 8** and **9** indicate that the present method can accurately reproduce the  
16 reference results by the correction of the cross section without explicit consideration of  
17 geometry deformation.

18 (Figure 7 Comparison of pin-by-pin fission rate (pin array within the yellow rectangle in  
19 Figure 6, from assembly A to E) )

20 (Figure 8 Perturbation of pin-powers due to increased gap size (fuel rods within the horizontal  
21 frame in Figure 6) )

22 (Figure 9 Perturbation of pin-powers due to increased gap size (fuel rods within the vertical  
23 frame in Figure 6) )

24

### 25 3. Conclusion

26 A simplified treatment for increased assembly gap of offset fuel assemblies due to

1 bowing is proposed. In the present method, nominal (non-offset) geometry is used while the  
2 cross section of the gap region is corrected to incorporate the variation of gap size. The gap  
3 size or the average chord length of a gap region is preserved in order to maintain the  
4 transmission probability. Verification results in the single assembly geometries and the 5x5  
5 assembly geometry indicate that the present method accurately reproduces the reference  
6 results obtained by explicit consideration of the offset geometry.

7       Since the present method does not require any geometry change, it will be a convenient  
8 candidate for high-fidelity core simulators that explicitly consider the heterogeneous geometry.  
9 Treatment of gap size variation along axial direction due to three-dimensional bowing of fuel  
10 assembly is difficult especially for core analysis codes utilizing extruded geometry for axial  
11 direction. The present method can offer a simple modeling approach in such situation.

12       In this paper, the validity of the proposed method is verified by a typical situation.  
13 Verification in other conditions (*e.g.*, use of different energy group structures, transport or  
14 diffusion method, gap size variation along axial direction) will be desirable. Effect of  
15 increased or decreased gap size on effective cross sections (*e.g.*, capture cross section of  $^{238}\text{U}$ )  
16 is not taken into account in this study. Investigation on this topic will be an interesting future  
17 task.

18

## 19 **References**

- 20 [1] Fetterman R, Franceschini F. Analysis of PWR Assembly Bow. Proc. PHYSOR 2008;  
21 2008 Sep.14-19; Interlaken(Switzerland). [CD-ROM]
- 22 [2] Franzen A. Evaluation of Fuel Assembly Bow Penalty Peaking Factors for Ringhals 3  
23 based on a Cycle Specific Core Water Gap Distribution. Master Thesis, UPTEC ES 17  
24 037; 2017; Uppsala University.
- 25 [3] Berger J. Impact of Fuel Assembly Bowing on the Power Density Distribution and its  
26 Monitoring in Siemens/KWU-PWR. Master Thesis, *TRITA-FYS 2017:60*; 2017; KTH.

- 1 [4] Bahadir T, Rodes J, Knott D. CMS Assembly Bow Model, 2017, Studsvik Scandpower.
- 2 [5] Franceschini F, Fetterman R, Little D, Modification of the ANC Nodal Code for Analysis  
3 of PWR Assembly Bow. Proc. PHYSOR 2008; 2008 Sep.14-19; Interlaken(Switzerland).  
4 [CD-ROM]
- 5 [6] Joo HG, Cho JY, Kim KS, Lee CC, Zee SQ. Methods and Performance of a  
6 Three-dimensional Whole-core Transport Code DeCART. Proc. PHYSOR 2004; 2004,  
7 Apr. 25-29; Chicago(IL). [CD-ROM].
- 8 [7] Kochunas B, Collins B, Jabaay J, Downar T, Martin W. Overview of Development and  
9 Design of MPACT: Michigan Parallel Characteristics Transport Code. Proc. M&C2013;  
10 2013 May.5-9; Sun Valley(ID). [CD-ROM]
- 11 [8] Ryu M, Junga YS, Cho HH, Joo HG. Solution of the BEAVRS Benchmark using the  
12 nTRACER Direct Whole Core Calculation Code. J. Nucl. Sci. Technol. 2015; 52, 961.
- 13 [9] Yamamoto A, Giho A, Kato Y, Endo T. GENESIS - A Three-dimensional Heterogeneous  
14 Transport Solver based on the Legendre Polynomial Expansion of Angular Flux method.  
15 Nucl. Sci. Eng., 2017; 186, 1.
- 16 [10] Kosaka S, Saji E, Transport Theory Calculation for a Heterogeneous Multi-Assembly  
17 Problem by Characteristics Method with Direct Neutron Path Linking Technique. J. Nucl.  
18 Sci. Technol. 2000; 37, 1015.
- 19 [11] Rochman D, Mala P, Ferroukhi H, Vasiliev A, Seidl M, Janin D, Li J. Bowing Effects  
20 on Power and Burn-up Distributions for Simplified full PWR and BWR Cores. Proc. M&C  
21 2017; 2017 Apr.16-20; Jeju, Korea. [USB-DRIVE].
- 22 [12] Yamamoto A, Kitamura Y, Yamane Y. Approximate Treatment of Thermal Expansion  
23 Effect in Lattice Transport Calculations. J. Nucl. Sci. Technol., 2004; 41, 1003.
- 24 [13] Reed M, Smith K, Forget B. "Virtual density" and Traditional Boundary Perturbation  
25 Theories: Analytic Equivalence and Numeric Comparison, Ann. Nucl. Energy, 2018; 112,  
26 531.

1 [14] Cho NZ, Benchmark Problems in Reactor and Particle Transport Physics. 2000;  
2 <http://nurapt.kaist.ac.kr/benchmark/>.

3

4

## Figure captions

- Figure 1. Layout of MOX fuel assembly and gap water
- Figure 2. Perturbation of pin-power distribution due to increased assembly gap size (unit:%, single assembly geometry)
- Figure 3. Difference of pin-by-pin fission rate obtained by the reference and the present methods (unit:%, single assembly geometry)
- Figure 4. Comparison of pin-by-pin fission rate (Eastern boundary, from North-East corner to South-East corner)
- Figure 5. Comparison of pin-by-pin fission rate (Southern boundary, from West-South corner to East-South corner)
- Figure 6. 5x5 assembly geometry with offset fuel assemblies
- Figure 7. Comparison of pin-by-pin fission rate (pin array within the yellow rectangle in Figure 6, from assembly A to E)
- Figure 8. Perturbation of pin-powers due to increased gap size (fuel rods within the horizontal frame in Figure 6)
- Figure 9. Perturbation of pin-powers due to increased gap size (fuel rods within the vertical frame in Figure 6)

**Table 1** Thickness of gap water around a fuel assembly (unit: cm)

Case	East	North	West	South
Nominal (E0.1-S0.1)	0.1	0.1	0.1	0.1
E0.1-S0.2	0.1	0.1	0.1	0.2
E0.1-S0.3	0.1	0.1	0.1	0.3
E0.2-S0.2	0.2	0.1	0.1	0.2
E0.3-S0.3	0.3	0.1	0.1	0.3

**Table 2** Variation of k-infinity due to increased gap size

Geometry	K-infinity		
	Reference (Increased gap with nominal XS)	Present (Nominal gap with corrected XS)	Difference
Nominal (E0.1-S0.1)	1.180241	-	-
E0.1-S0.2	1.181430	1.181412	-0.002%
E0.1-S0.3	1.182516	1.182492	-0.002%
E0.2-S0.2	1.182605	1.182566	-0.003%
E0.3-S0.3	1.184732	1.184677	-0.005%



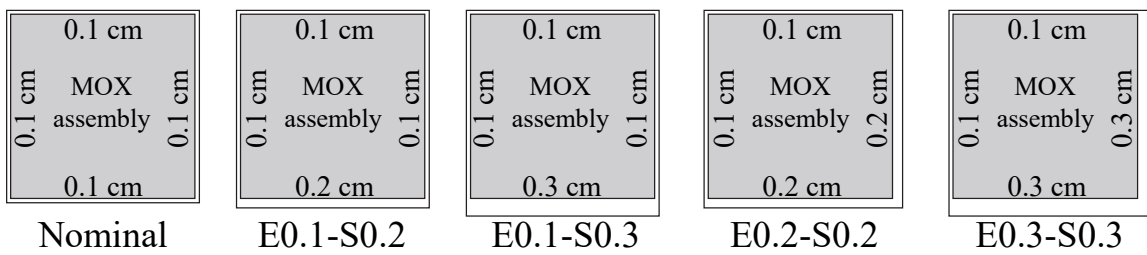
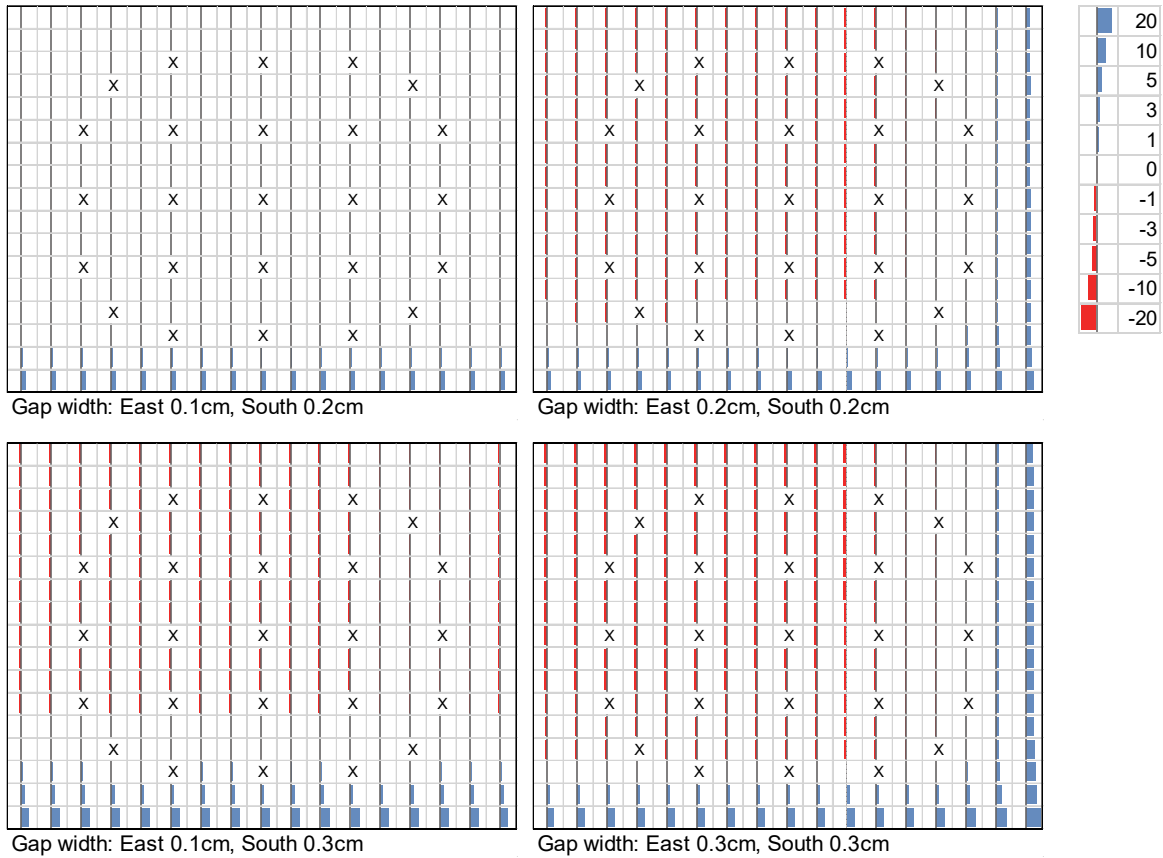


**Figure 1.** Layout of MOX fuel assembly and gap water

A. Yamamoto:

A simple treatment of increased gap due to fuel assembly bowing through correction of cross sections

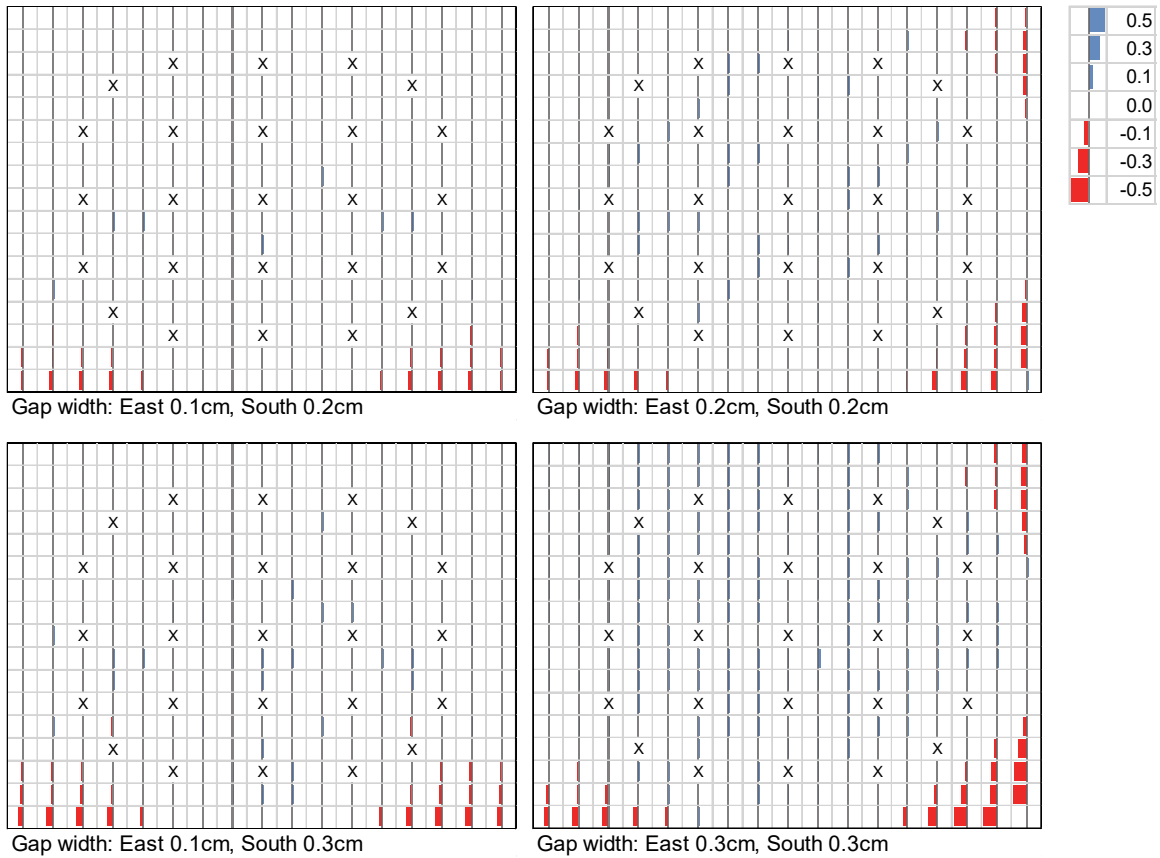


**Color  
Print**

**Figure 2.** Perturbation of pin-power distribution due to increased assembly gap size (unit:%, single assembly geometry, X indicates instrumental or guide thimbles)

A. Yamamoto:

A simple treatment of increased gap due to fuel assembly bowing through correction of cross sections



**Color  
Print**

**Figure 3.** Difference of pin-by-pin fission rate obtained by the reference and the present methods (unit:%, single assembly geometry, X indicates instrumental or guide thimbles)

A. Yamamoto:

A simple treatment of increased gap due to fuel assembly bowing through correction of cross sections

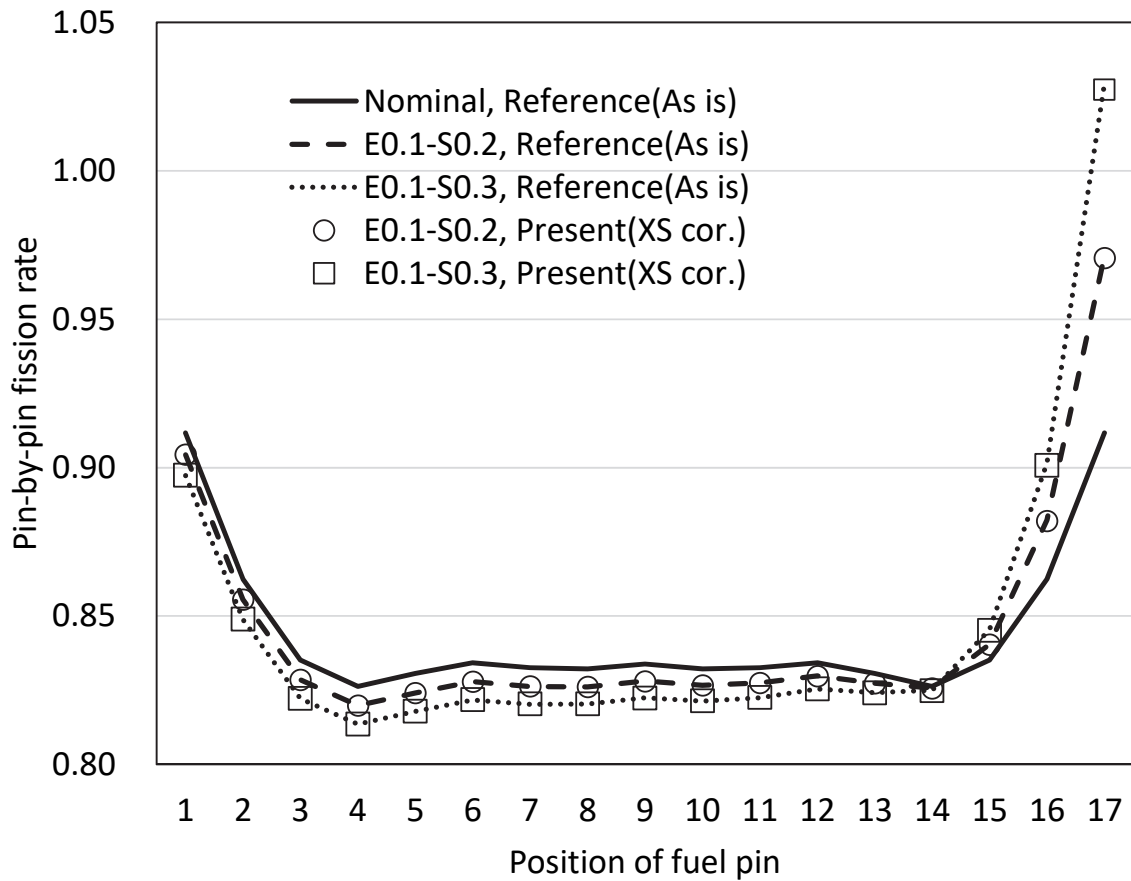


**Figure 4.** Comparison of pin-by-pin fission rate (Eastern boundary, from North-East corner to South-East corner)

A. Yamamoto:

A simple treatment of increased gap due to fuel assembly bowing through correction of cross sections

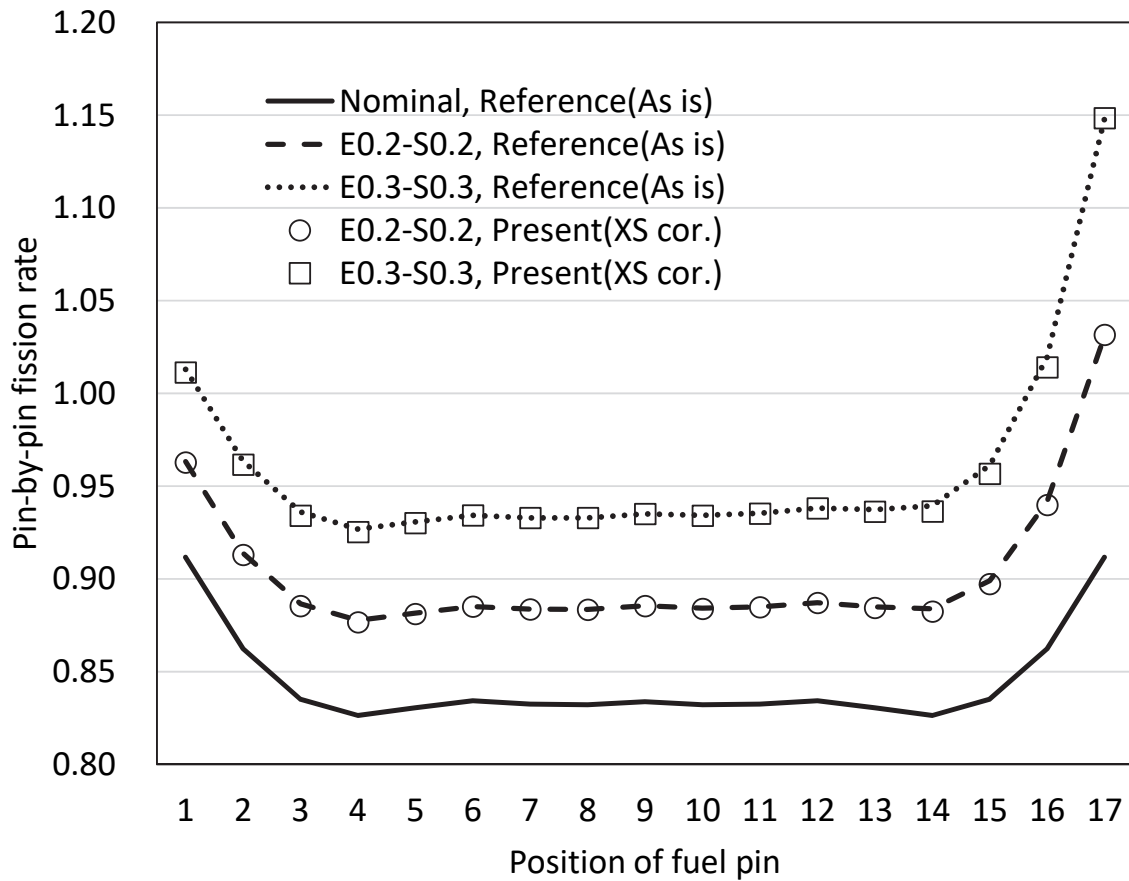
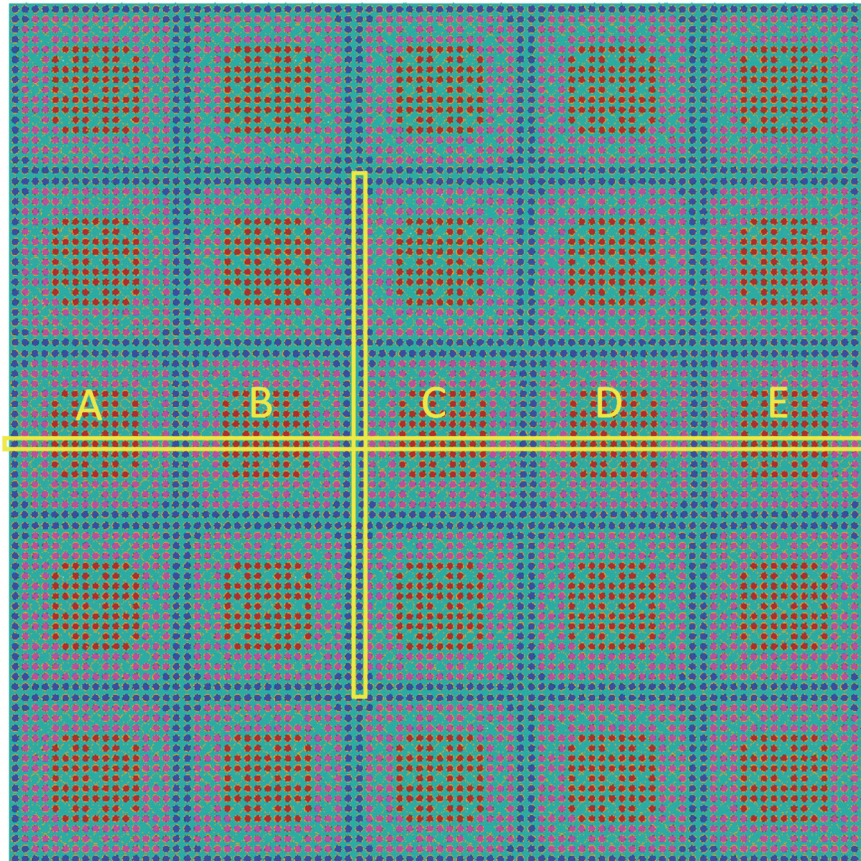


**Figure 5.** Comparison of pin-by-pin fission rate (Southern boundary, from West-South corner to East-South corner)

A. Yamamoto:

A simple treatment of increased gap due to fuel assembly bowing through correction of cross sections



**Color  
Print**

**Figure 6.** 5x5 assembly geometry with offset fuel assemblies

A. Yamamoto:

A simple treatment of increased gap due to fuel assembly bowing through correction of cross sections

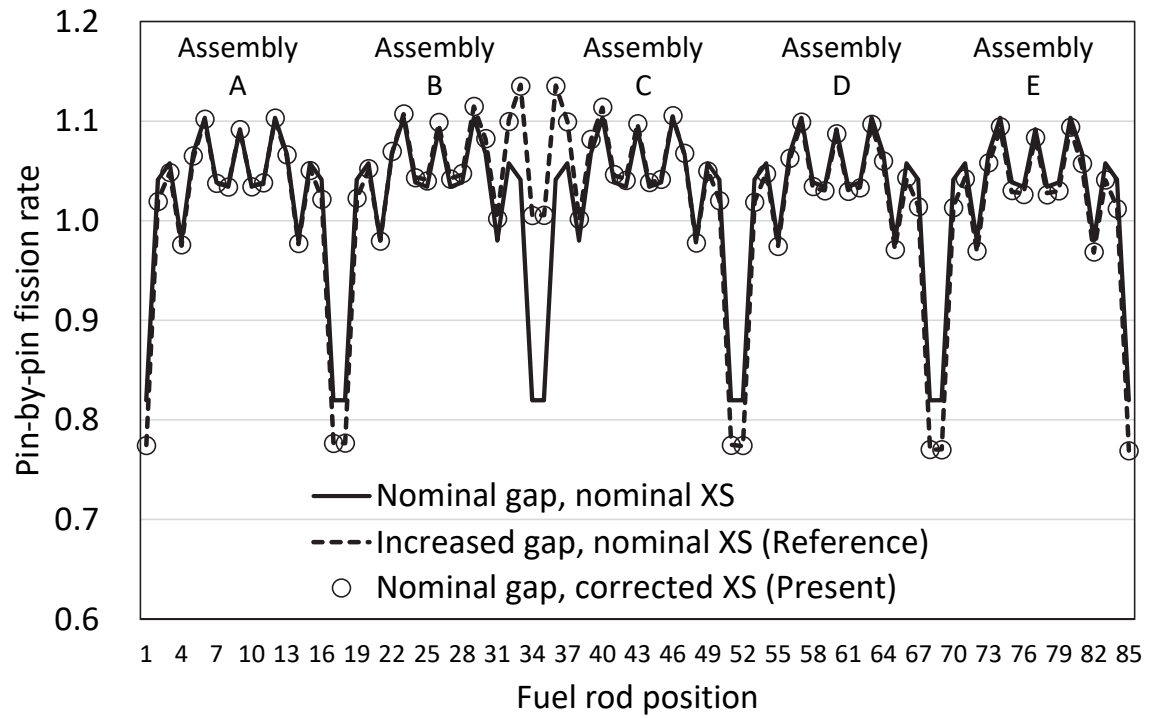


**Figure 7.** Comparison of pin-by-pin fission rate (pin array within the yellow rectangle in Fig.6, from assembly A to E)

A. Yamamoto:

A simple treatment of increased gap due to fuel assembly bowing through correction of cross sections

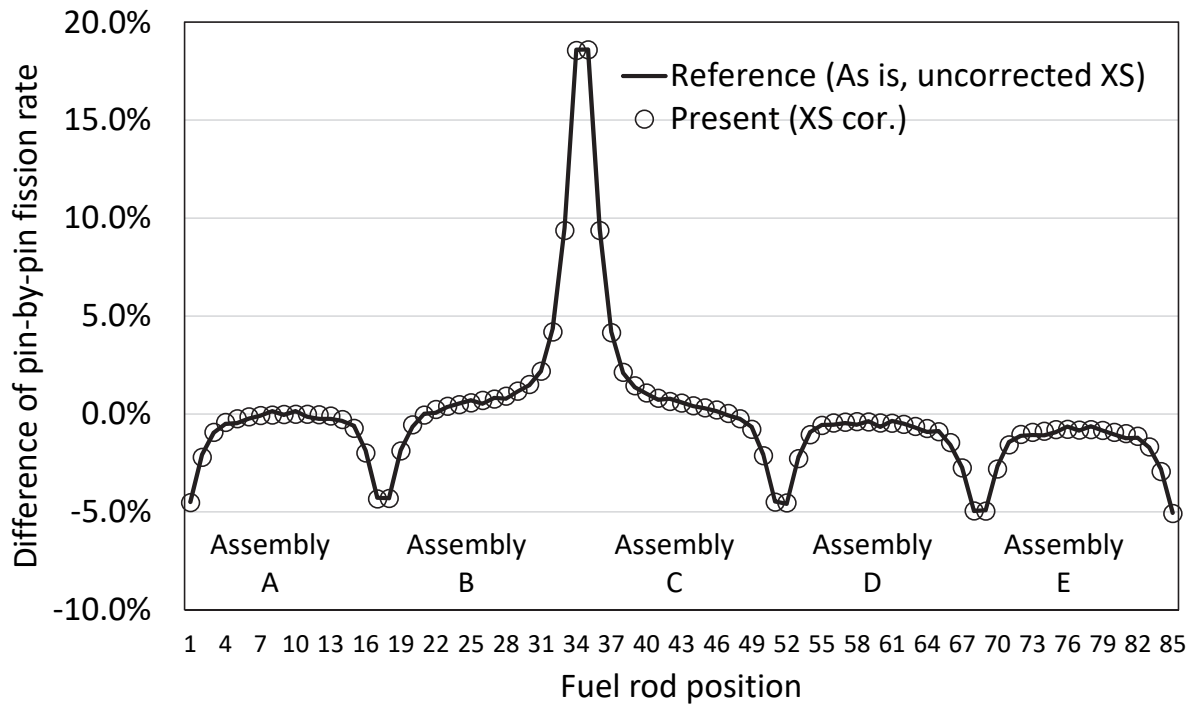


**Figure 8.** Perturbation of pin-powers due to increased gap size (fuel rods within the horizontal frame in Figure 6)

A. Yamamoto:

A simple treatment of increased gap due to fuel assembly bowing through correction of cross sections



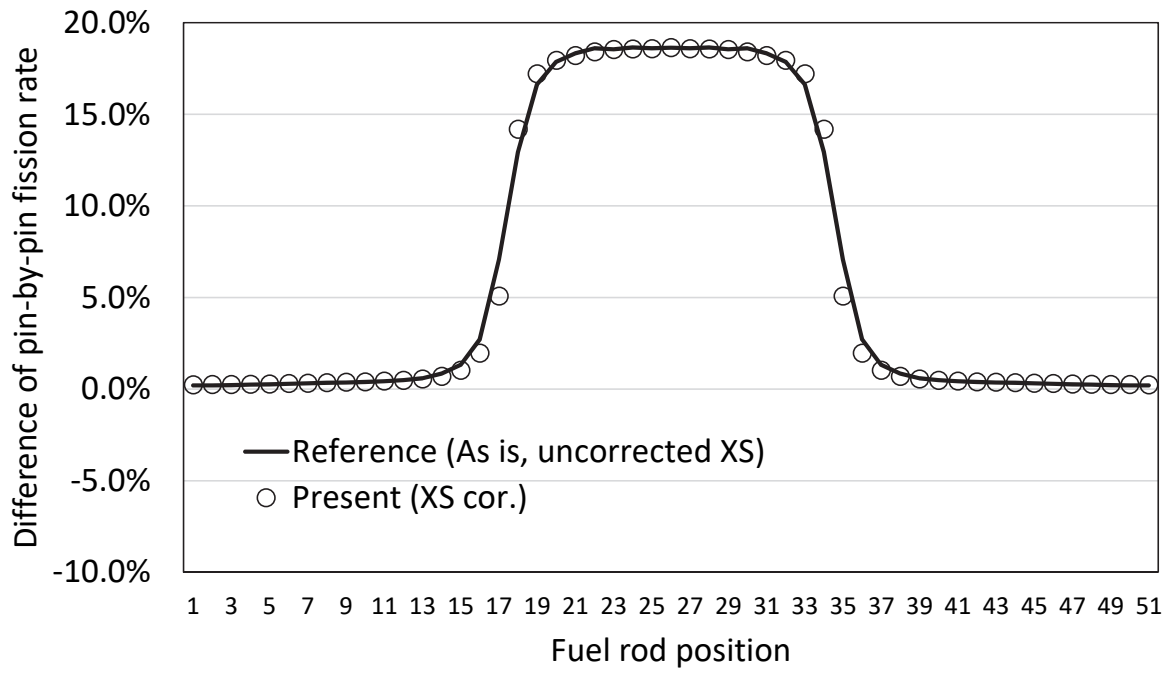


**Figure 9.** Perturbation of pin-powers due to increased gap size (fuel rods within the vertical frame in Figure 6)

A. Yamamoto:

A simple treatment of increased gap due to fuel assembly bowing through correction of cross sections